Simulating lake ice phenology using a coupled atmosphere-lake model at Lake Nam Co, a typical deep alpine lake on the Tibetan Plateau

Xu Zhou[1], Binbin Wang[1], Xiaogang Ma[2], Zhu La[3], and Kun Yang[2]

[1]State Key Laboratory of Tibetan Plateau Earth System and Resource Environment, Institute of Tibetan Plateau Research, Chinese Academy of Sciences, Beijing 100101, China

[2]Department of Earth System Science, Ministry of Education Key Laboratory for Earth System Modelling, Institute of Global Change Studies, Tsinghua University, Beijing 100084, China

[3]School of Ecology and Environment, Tibet University, Lhasa 850000, China

Correspondence to: Binbin Wang (wangbinbin@itpcas.ac.cn)

Abstract. Simulating the ice phenology of deep alpine lakes is important and challenging in coupled atmosphere-lake models. In this study, the Weather Research and Forecasting (WRF) model, coupled with two lake models, the fresh-water lake model (WRF-FLake) and the default lake model (WRF-Lake), was applied to lake Nam Co, a typical deep alpine lake located in the centre of the Tibetan Plateau, to simulate its lake ice phenology. Due to the large errors in simulating lake ice phenology, related key parameters and parameterizations were improved in the coupled model based on observations and physics-based schemes. By improving the momentum, hydraulic and thermal roughness length parameterizations, both the WRF-FLake and the WRF-Lake models reasonably simulated the lake freeze-up date. By improving the key parameters associated with shortwave radiation transfer process when lake ice exists, both models generally simulated the lake break-up date well. Compared with WRF-Lake without improvements, the coupled model with both revised lake models significantly improved the simulation of lake ice phenology. However, there were still considerable errors in simulating the spatial patterns of freeze-up and break-up dates, implying that significant challenges in simulating the lake ice phenology still exist in representing some important model physics, including lake physics such as grid-scale water circulation, and atmospheric processes such as snowfall and surface snow dynamics. Therefore, this work can provide valuable new implications for advancing lake ice phenology simulations in coupled models and the improved model also has practical application prospects in weather and climate forecasts.

1 Introduction

Alpine lakes are one key land cover type on the TP. These lakes serve as a main water supply of the TP, i.e., the 'Asia water tower' [*Xu et al.*, 2008], with a total coverage of more than 47000 km[2] [*Zhang et al.*, 2019; *Zhang et al.*, 2014]. Therefore, alpine lakes play a crucial role in local and regional climate through thermal and hydrological cycles in the Earth system. For example, alpine lakes can influence the precipitation over lakes and surroundings through both dynamic and thermal

processes [*Dai et al.*, 2018b; *Su et al.*, 2020; *Wu et al.*, 2019; *Yang et al.*, 2022; *Yao et al.*, 2021; *Zhao et al.*, 2022]. An accurate simulation of lake climatic impacts is the premise of deriving reasonable forecasting results in climate models. However, there are still large uncertainties in the parameterizations of the associated physical processes.

Lakes over mid-high latitudes undergo seasonal freeze-thaw cycles, which show significantly different characteristics
35   between deep and shallow lakes. Due to the large contrast in heat capacity associated with the large water storage per unit area, deep lakes often show significantly different ice phenology characteristics compared to shallow lakes and surrounding land areas. Many alpine lakes are deep lakes with average depths greater than 20 metres, such as Qinghai Lake, Nam Co, and Selin Co [*Guo et al.*, 2016; *Li et al.*, 2016; *Wang et al.*, 2009]. The ice phenology seasonality of alpine lakes can influence not only the lake water budget, but also the seasonality of local and regional climates. For example, long-term freeze-up can
40   maintain water levels by preventing evaporation losses in lakes [*Lei et al.*, 2018]. The surface evaporation of lakes will significantly increase during the cold ice-free period due to the strong turbulent mixing of lake water, which can provide appropriate moisture conditions for snowfall events.

The freeze-up date of a lake depends on the balance of energy storage and release of lake water. Turbulent heat fluxes play an important role in simulating the energy stored by lake water, and thus influence the freeze-up date [*Ma et al.*, 2022; *Zhou*
45   *et al.*, 2023]. The parameterizations of lake surface turbulent heat fluxes may have large uncertainties [*Wen et al.*, 2016], while the formulations of radiation processes at the water surface are relatively stable. Thus, the physical schemes of the heat fluxes need to be accurately parameterized in numerical models. One key parameter in simulating the turbulent heat fluxes is the roughness length, which has been proven to play an important role in simulating the freeze-up date of Nam Co [*Ma et al.*, 2022]. The melting of lake ice mainly depends on solar radiation related processes [*Efremova and Pal'shin*, 2011; *Huang et*
50   *al.*, 2022], especially the shortwave processes for ice and water, which are closely related to the albedo and the extinction coefficient [*Kirillin et al.*, 2012; *Li et al.*, 2021]. The absorption of the shortwave at the ice surface, deep ice, and water underneath can result in different ice thicknesses and freeze-up dates [*Zhou et al.*, 2023].

Offline lake models show considerable ability to simulate the seasonal freeze-up and break-up dates of alpine lakes [*Dai et al.*, 2018a; *Huang et al.*, 2019a; *Huang et al.*, 2019b; *Li et al.*, 2021]. However, regional climate and weather forecasts, as
55   well as the lake effect can be achieved only through a coupled model. Therefore, the application and ability of coupled atmosphere-lake models for deep alpine lakes still needs to be further investigated, as highlighted in previous studies [*Su et al.*, 2020; *Wu et al.*, 2019; *Zhou et al.*, 2023]. It is more challenging for a coupled atmosphere-lake model to simulate the ice phenology of alpine lakes, because for offline simulation, the atmospheric forcing is prescribed from observation or reanalysis data, which is a strong constraint on model performance and usually has fatal disadvantages. For example, the
60   shortwave radiation above lake surface can be 100 W/m^{-2} stronger than that of the surrounding land due to the cloud hole effect [*Yao et al.*, 2023]. Thus, simulating lake ice phenology using a coupled model is necessary and important. Furthermore, a coupled model is more sensitive to key parameters and parameterizations, since the long-term integration will increase the model errors through the two-way exchange of energy and water between atmosphere and lake surface [*Zhou et al.*, 2023].

65   Therefore, in this work, the Weather Research and Forecasting (WRF) model coupled with two lake models, the fresh-water lake (FLake) model [*Mironov*, 2008] and the simplified Community Land Model (CLM) lake model [*Gu et al.*, 2015], was applied to a typical deep alpine lake, Nam Co. Noting that *Zhou et al.* [2023] proved by artificially adding a proper scaling factor on fraction velocity can better simulate the surface turbulent heat fluxes and ice phenology of Nam Co. However, such sensitivity method is hard to be regarded as advancing a climate model. The current work is an extension of that work by

70   revising key parameters and improving key parameterizations using observations and physics-based schemes to better simulate lake energy circulations. The main objectives were to improve the simulation of the lake ice phenology in the WRF model for deep alpine lakes and to propose important challenges more accurately simulating the lake ice phenology characteristics in coupled atmosphere-lake models. This work is expected to provide a better model version and to provide valuable guidance in applying and advancing climate models for deep alpine lakes.

75   **2 Study region and data**

2.1 Study region

The target lake is Nam Co (Figure 1a), which is a typical deep lake located in the central TP at approximately 30.7ºN, 90.6ºE. It covers an area of more than 2000 km^2 and has an average depth of approximately 40 m [*La et al.*, 2016]. Under global warming, the lake water level has experienced a rapid increase since the 1990s due to the increase in precipitation, and the

80   growing water supplied by melting snow and glaciers within the basin [*Lei et al.*, 2014; *Lei et al.*, 2013; *Zhang et al.*, 2020].
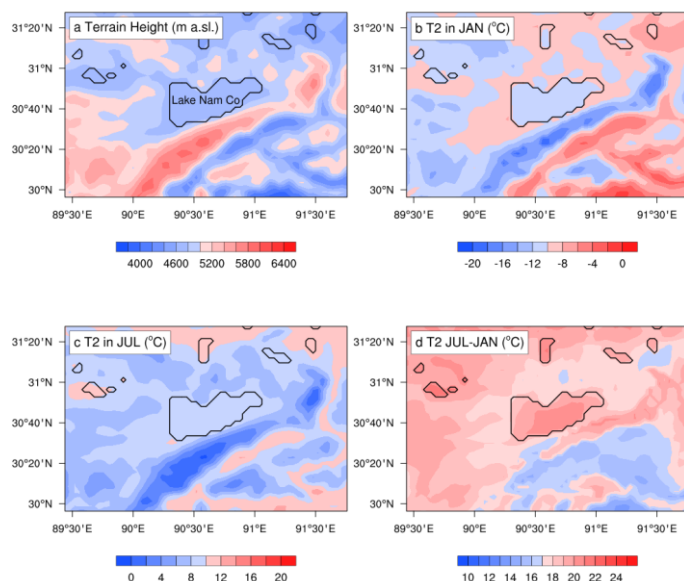

Figure 1: (a) The study region and the simulation domain of the current study, with Nam Co located in the centre; black contour lines denote the lake mask; colour shading denotes the terrain elevation (meters above sea level); the 2m air

85   temperature (T2 in °C) in (b) January and (c) July (colour shading) derived from default WRF simulation; and the difference of T2 (°C) between July and January (colour shading).

Seasonally, the study region undergoes large temperature variability with a cold air temperature generally below 0 °C in January (Figure 1b) and a warm air temperature generally above 0 °C in July (Figure 1c). Large air temperature difference between the two months can reach more than 22 °C (Figure 1d), indicating a strong seasonality, and thus the physical

90   processes related with ice-water phase change may play an important role in the water and energy cycles within the study region. Lakes over this region undergoes typical freezing and melting cycles.

2.2 Data

The lake water temperature (TW) data observed in Nam Co cover a period from November 2011 to June 2014 [*Wang*, 2020]. These data are the daily average water temperature data at different depths (from 3 m to more than 60 m) and were obtained

95   through field monitoring. The data were continuously recorded by deploying a water quality multi-parameter sonde and temperature thermistors in the water. The daily average water temperature was calculated based on the original observed data. In the current work, the TW was used for model evaluation. Only the data from the period of 1st July 2013 to 30nd June 2014 were used, because the station data after 1st July 2014 is not available due to the instrument damage.

The MODIS lake surface temperature (LST) product was used for comparison with the model results. The 0.05 ° Aqua and

100   Terra daily datasets were used in the current study [*Wan et al.*, 2015]. For a fair comparison, the MODIS data were interpolated to the model grid by the area weighted method. Due to the contamination by clouds, MODIS has missing observations at a considerable number of pixels. Thus, the mean LSTs were calculated and compared with those from each simulation. For quality control, the LSTs with a fraction of missing observations larger than 90% were removed. Nonetheless, there were still some outliers especially for nighttime data. Additionally, the land-water mixed pixels (the nearest two pixels

105   to land) in MODIS were excluded and a total of 1574 grids were used.

ERA_interim reanalysis data [*Dee et al.*, 2011] from the European Centre for Medium-Range Weather Forecasts (ECMWF) was used for model initial and lateral boundary forcing conditions. It was developed based on the Integrated Forecasting System (IFS) model assimilating multisource observations. This data has a resolution of approximately 80 km (T255 spectral) on 60 vertical levels from the surface up to 0.1 hPa.

110   ## 3 Model description and setup

3.1 WRF model and model setup

The coupled atmosphere-lake model used in the current study was the WRF model coupled with the FLake model and the simplified CLM lake model, defined as WRF-FLake and WRF-Lake hereafter. The default WRF was developed by NCAR. It is a nonhydrostatic model with multiple schemes in the planetary boundary layer, the land surface model, the cloud

115 microphysics, the cumulus convection, the orographic drag and so on. In this study, WRF3.9 [*Skamarock et al.*, 2008] was
applied to the TP region.

Figure 1a shows the simulation domain, covering Nam Co and the surrounding land. The WRF model setup is generally
consistent with *Zhou et al.* [2023], with a horizontal grid spacing of 0.04º (approximately 4.5 km), which is identified as
convective permitting. The lateral boundary conditions were provided at six hourly intervals. The simulations were
120 integrated for two years from 1st July 2013 to 30th June 2015. The model was initialized at 00:00 on 1st July 2013 using
MODIS observations. Based on previous studies over the TP, a turbulent orographic form drag scheme was used to represent
the subgrid orographic drag [*Zhou et al.*, 2017; *Zhou et al.*, 2021], the Dudhia scheme [*Dudhia*, 1989] and the RRTM
[*Mlawer et al.*, 1997] were used for shortwave and longwave radiation transfer, the Modified Thompson scheme [*Thompson
et al.*, 2008] was used for the microphysics, the Noah-MP [*Niu et al.*, 2011; *Yang et al.*, 2011] was used for the land surface
125 processes, and the Mellor–Yamada–Janjic turbulent kinetic energy scheme [*Janjic*, 2001; *Mellor and Yamada*, 1974] was
used for the planetary boundary layer.

Three experiments were designed in the current study. One used the WRF coupled with the default lake model without
revisions of key lake parameters and parameterizations, which was defined as the control run (WRF-Ctrl). The other two
used WRF coupled with the revised FLake model and revised default lake model, defined as WRF-FLake run and WRF-
130 Lake run. The unrevised version of the WRF-FLake model was not selected as a control run because it had difficulties
simulating the ice phenology characteristics, i.e. a considerable number of lake grids never freeze-up, and/or never break-up
after freeze-up [*Zhou et al.*, 2023]. In this study, two lake models were used to demonstrate the universality of the revisions
in parameterization schemes in improving the simulation of lake ice phenology characteristics.

3.2 Lake models and model setup

In this section, we introduce the two one-dimensional lake models that have been coupled to WRF as the lake scheme to
reflect the climatic effects of lake processes. The lake model setup in the coupled model is also introduced.

One is the FLake, which is a freshwater model developed by *Mironov* [2008]. It is a two-layer model with an upper mixed
layer and a thermocline layer in which the water temperature is parameterized by self-similarity theory. One key feature of
140 FLake is that the mixed layer depth is parameterized by diagnosing the water stability conditions, which is different from the
finite differential model in which the energy exchange is parameterized by a turbulent mixing ratio. FLake was coupled with
WRF by *Zhou et al.* [2023] to perform sensitivity studies of key physical processes in simulating lake ice phenology. This
study used the same version.

The other lake model is the default one in WRF, which is a simplified version of the CLM lake model. It is a finite
145 differential model that was originally designed for shallow lakes. It has ten vertical layers and the water turbulent mixing
ratio is empirically set to a constant between the layers. The CLM lake model is simplified and coupled with WRF by *Gu et
al.* [2015] to describe lake processes and effects on the atmosphere.

Previous studies have shown that using the default settings in lake models can lead to considerable errors in the simulations [*Huang et al.*, 2019a; *Ma et al.*, 2022; *Zhou et al.*, 2023]. Thus, some key parameters and physical schemes were revised
150 based on previous studies. For both lake model setups in the coupled model, the lake depth was set to the average value of 40 m for lake grids, which was consistent with the offline study by *La et al.* [2016]. Thus, the lake status can be initialized by their simulation results to save computational expense for long-time spin up in the coupled model. Noting that both lake models used in the current study are one-dimensional models, such a setup with identical depth for all grids can, to some extent, reflects the horizontal energy mixing associated with lake water circulation. The water extinction was set to 0.12
155 according to *Wang et al.* [2009] and *Huang et al.* [2019a]. The temperature at maximum water density was set to 3.5℃ according to *Wang et al.* [2019b] and *Wu et al.* [2019].

3.3 Model improvements and limitations

In the Default WRF-Lake model, the momentum, hydraulic and thermal roughness lengths were set to constant values of 0.001. In the default FLake model, the roughness length for momentum (z_{0m}) is parameterized as follows:

160
$$z_{0m} = \alpha \times \frac{u_*^2}{g} \tag{1}$$

where α is the Charnock number calculated by $\alpha = 0.0012 + 0.7 \times (1/1000 \times (u^2)/g)$, with u is the surface wind speed; u_* is the surface friction velocity in m/s; $g = 9.8$ m/s^2 is the gravitational acceleration constant. Then, the hydraulic roughness length z_{0q} is further parameterized as follows:

$$z_{0q} = z_{0m} \times \exp\left(-C_k \times \left(4.0 \times \left(\frac{u_*^3}{g \times \nu}\right)^{0.5} - 4.2\right)\right) \tag{2}$$

165 where $C_k = 0.4$ is the Von Karman constant; ν is the kinematic viscosity of air. And thermal roughness length z_{0h} is further parameterized as follows:

$$z_{0h} = z_{0m} \times \exp\left(-C_k \times \left(4.0 \times \left(\frac{u_*^3}{g \times \nu}\right)^{0.5} - 3.2\right)\right) \tag{3}$$

The above formulation is used in *Zhou et al.* [2023], which introduced large model errors in simulating lake ice freeze-up time. Because such a parameterization simulated too weak turbulent heat fluxes, and these fluxes have too enlarged 1.5 times
170 to improvement the model performance. Nevertheless, such artificial method lacks physical basis and is model dependent. In the current study, different from such methods, an observation-based roughness length scheme for open water [*Wang et al.*, 2019a] were used for both WRF-Lake and WRF-FLake, which have been proven to better simulate the heat fluxes and lake freeze-up date in WRF-Lake [*Ma et al.*, 2022]. z_{0m} is parameterized as follows:

$$z_{0m} = \alpha \times \frac{u_*^2}{g} + R_r \times \frac{\nu}{u_*} \tag{4}$$

175 where $\alpha = 0.031$, $R_r = 0.54$, for lake Nam Co; ν is the kinematic viscosity of air; u_* is the surface friction velocity in m/s; $g = 9.8$ m/s^2 is the gravitational acceleration constant; and $R_e = u_* z_{0m}/\nu$ is the roughness Reynolds number. Then, the hydraulic and thermal roughness lengths z_{0q} and z_{0h} are further parameterized as follows:

$$z_{0q} = z_{0h} = z_{0m} \times \exp(-2.67 \times R_e^{0.25} + 0.57) \tag{5}$$

where $R_e = u_* z_{0m}/\nu$ is the Reynolds number.

180 In Default WRF-Lake model, the division of the vertical layers of lake is four [*Ma et al.*, 2022]. In the current work, to better simulate the lake ice break-up date, the division of the vertical layers of the lake in WRF-Lake was revised to ten layers according to CLM4.5. The default ice albedo in WRF-Lake is 0.6. In the current study, it was set to 0.55 with the consideration that 0.5-0.6 is the most distributed ranges of albedo observations for the Lake Nam Co, as investigated in *Li et al.* [2018]. In WRF-FLake, the albedo α is parameterized by the ice surface temperature as follows:

185 $$\alpha = \alpha_{max} - (\alpha_{max} - \alpha_{min})\exp(-95.6(T_f - T_s)/T_f) \tag{6}$$

where α_{max} and α_{min} are the maximum and minimum ice albedo, respectively, $T_f = 273.15$ is the temperature at the freezing point, and T_s is the ice surface temperature. In *Zhou et al.* [2023], the default values of α_{max} and α_{min} were set to 0.2 and 0.1 respectively, with the consideration of ice albedo variance under snow-free conditions. Nevertheless, the value of 0.2 is too small under all conditions (when snow often appears), as observed from satellite [*Li et al.*, 2018]. Therefore, in the

190 current study, α_{max} is revised to 0.75 based on satellite observation [*Li et al.*, 2018]. Such treatment of lake surface albedo is a matter of expediency due to the model disadvantage in modelling snow fall the associated snow cover over lake ice. Thus, the snow influence on lake-ice albedo is directly taken into account even the model cannot simulate enough snow fall. Additionally, considering the absorption of shortwave radiation at the ice surface is also an important parameter, it is revised to 0.65 according to a sensitivity study similar to that in *Zhou et al.* [2023].

195 The snow cover over lake ice can bring large uncertainties in the model, which will be discussed in Section 5. Thus, we decided to keep the original formulations of lake ice albedo formulations in both lake models but with empirical revisions as given above. However, this method may lead to some biases and accurately parameterizing the lake ice albedo during freeze-up was not feasible that could be caused by the models' limitations on snow-related processes as discussed in Section 5, and more substantial work is needed.

200 ## 4 Results and analysis

4.1 Surface heat flux and water temperature

Previous studies show that there are large uncertainties in simulating turbulent heat fluxes in lake models [*Wen et al.*, 2016] and thus play key roles in simulating the lake water temperature and lake freeze-up date [*Ma et al.*, 2022; *Zhou et al.*, 2023]. In contrast, other energy components at the lake surface are relatively more reasonably parameterized due to reliable

205 observations. For example, regarding shortwave and longwave radiation, the albedo for open water is approximately 0.08 and the emissivity is approximately 0.98. These two key parameters have low uncertainties and can be accurately estimated. Therefore, only the simulated turbulent heat fluxes and water temperature were investigated in this section.

Figure 2 shows the differences in daily mean sensible heat and latent heat derived from WRF-FLake and WRF-Lake minus WRF-Ctrl at Nam Co averaged over all lake grids for the study period. Compared with WRF-Ctrl, both WRF-FLake and

210 WRF-Lake show quite smaller differences in simulating the sensible heat (SH) for ice-free periods (Figure 2a), while they show considerable smaller negative differences in simulating the latent hear (LH) for ice-free periods especially within approximately one month before ice-on (Figure 2b), indicating that the LH is more sensitive to the improvements in the hydraulic and thermal roughness lengths parametrizations as introduced in section 3.2. The improved model WRF-FLake and WRF-Lake show quite good agreement with each other, because both models used the same parameterizations of

215 momentum and thermal roughness lengths (Section 3.2). Both WRF-FLake and WRF-Lake obviously show larger SH and LH in November-December than WRF-Ctrl due to the early ice-on in WRF-Ctrl model. Additionally, there are some differences at the initial stages of ice-on between the two improved models, which could be associated with differences in locations and numbers of grids that are freeze-up. Nevertheless, other thermal processes (such as water turbulent mixing) also play certain roles and caused different model performances in simulating SH, LH, and lake ice-on start time. Obviously,

220 the smaller LH during ice-free periods in both WRF-FLake and WRF-Lake simulations leads to a weaker water energy release, resulting in a late ice-on.

The SH and LH control the atmosphere-lake energy exchange and lake water energy storage, and thus influence the lake freeze-up date [*Ma et al.*, 2022; *Zhou et al.*, 2023]. In the following, the LST and water temperature profiles are compared with MODIS and station observations, respectively.
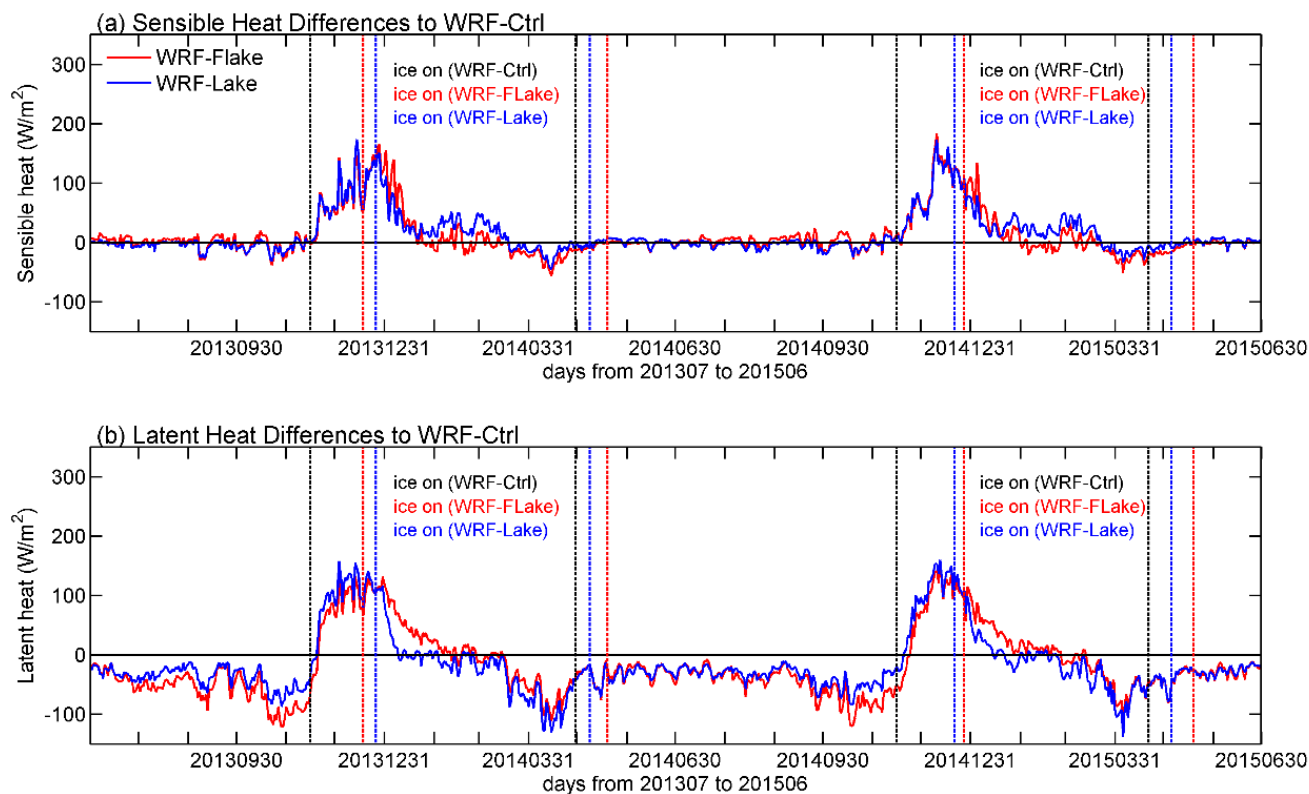
225

Figure 2: Differences in the daily mean (a) sensible heat and (b) latent heat simulated derived from WRF-FLake and WRF-Lake minus WRF-Ctrl at Nam Co averaged over all lake grids for the study period. The vertical lines show the first/last days of ice occurrences in each simulation (black: WRF-Ctrl; red: WRF-FLake; blue: WRF-Lake).

Figure 3a shows the time series of mean LST biases in each simulation against MODIS data for the study period. WRF-Ctrl obviously show cold biases during ice-free periods. These cold biases are obviously alleviated in both the WRF-FLake and the WRF-Lake runs. Considering the uncertainties in the MODIS products, that is, there are obvious unreliable underestimations of night time LST for alpine lakes including Nam Co [La et al., 2022], warmer biases in LST are expected. Larger cold biases in WRF-Ctrl occurs in November-December due to the early ice-on, which is significantly improved in the WRF-FLake and the WRF-Lake runs. At the time of early ice-on in these two runs, the simulated LST also show cold biases. The reason could be that for MODIS, only ice-free pixels were averaged because the freeze-up pixels were hard to distinguish between lake surface or cloud top, which also explains the continuous missing observations of MODIS during lake freeze-up. Figure 3b shows the differences in the daily mean LST derived from WRF-FLake and WRF-Lake minus WRF-Ctrl for the study period. WRF-FLake and WRF-Lake runs obviously have warmer LST during ice-free period, which can be explained by the stronger cooling effect due to the larger LH release as shown in Figure 2b. The largest LST differences in WRF-FLake and WRF-Lake in November-December are caused by the early ice-on in the WRF-Ctrl.

9
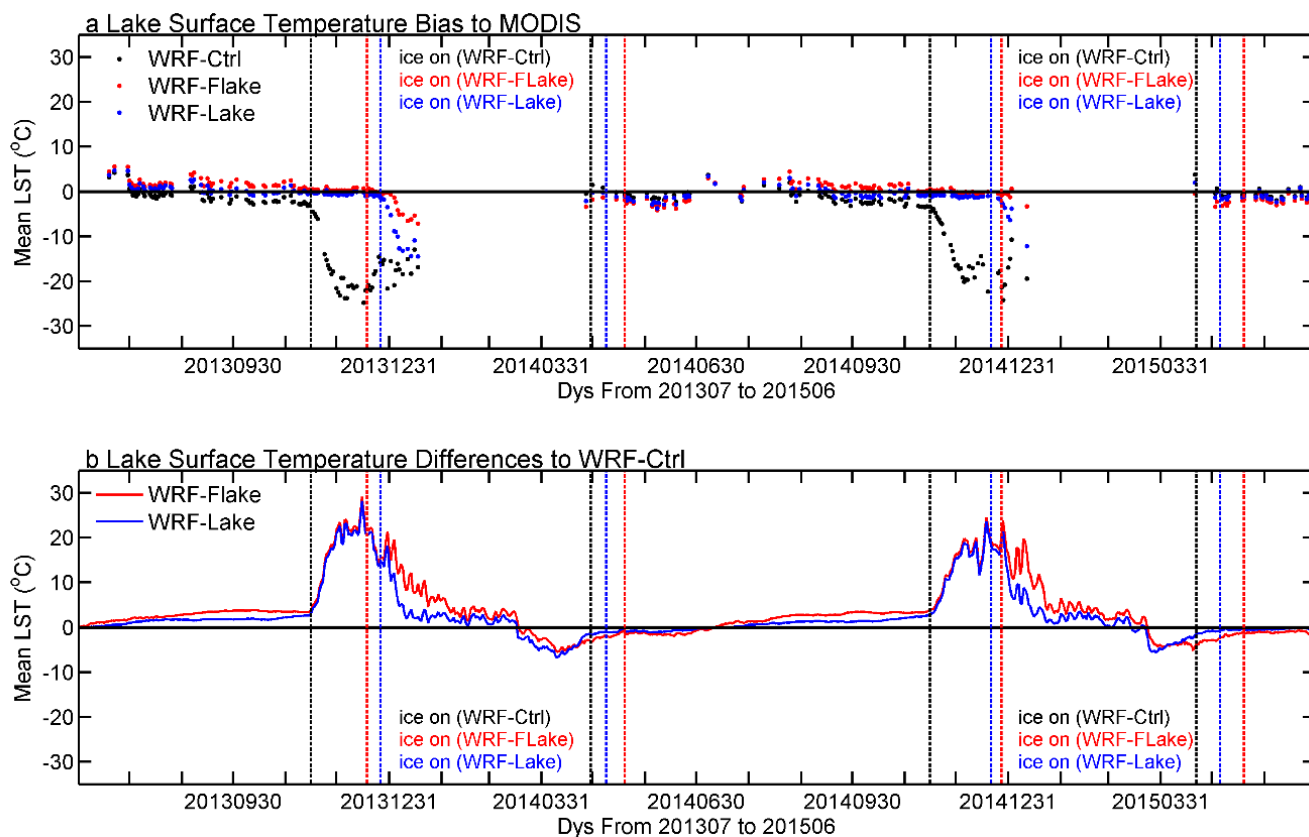
Figure 3: (a) The biases in daily mean LST to MODIS in each simulation (black: WRF-Ctrl; red: WRF-FLake; blue: WRF-Lake) for the study period, and (b) the differences in the daily mean LST derived from WRF-FLake and WRF-Lake minus WRF-Ctrl for the study period. The vertical lines show the first/last days of ice occurrences in each simulation (black: WRF-Ctrl; red: WRF-FLake; blue: WRF-Lake).

Figure 4 shows the observed and simulated lake water temperature profiles. Only the data from the period of 1st July 2013 to 30nd June 2014 were used, because the station data after 1st July 2014 were not available due to instrument damage. All the simulations can generally simulate the seasonality of the water temperature with the maximum occurring in August-September, and the minimum occurring in winter and early spring. Consistent with the investigation in *Wang et al.* [2019b], obvious water stratification lasts from July to late October, while the water body is sufficiently mixed after that time until May of the next year (Figure 4a). During the ice-on period, the thermal structure of the water column is weakly stratified rather than mixed [*La et al.*, 2021]. The stratification characteristics in the simulations generally agree well with the measurements (Figure 4b-c). Additionally, the mean bias and root mean square error (RMSE) are calculated (Figure 4d-e). The WRF-Ctrl and WRF-Lake runs show cold biases, especially at shallow layers, while WRF-FLake has smaller mean bias

errors (Figure 4d). By revising key parameters and improving key parameterizations of lake models, the cold biases can be

260 effectively alleviated. The RMSE in WRF-FLake is larger at deep layers, indicating a worse performance, and vice versa at

shallow layers (Figure 4e). The bias in WRF_FLake is smaller than that in WRF-Ctrl and WRF-Lake, while the RMSE is

larger for some layers. This could be associated with the differences in seasonal variation in the LST between the models and

observations. That is, WRF-FLake (Figure 4b) is much warmer in summer and colder in winter than is WRF-Lake (Figure 4c)

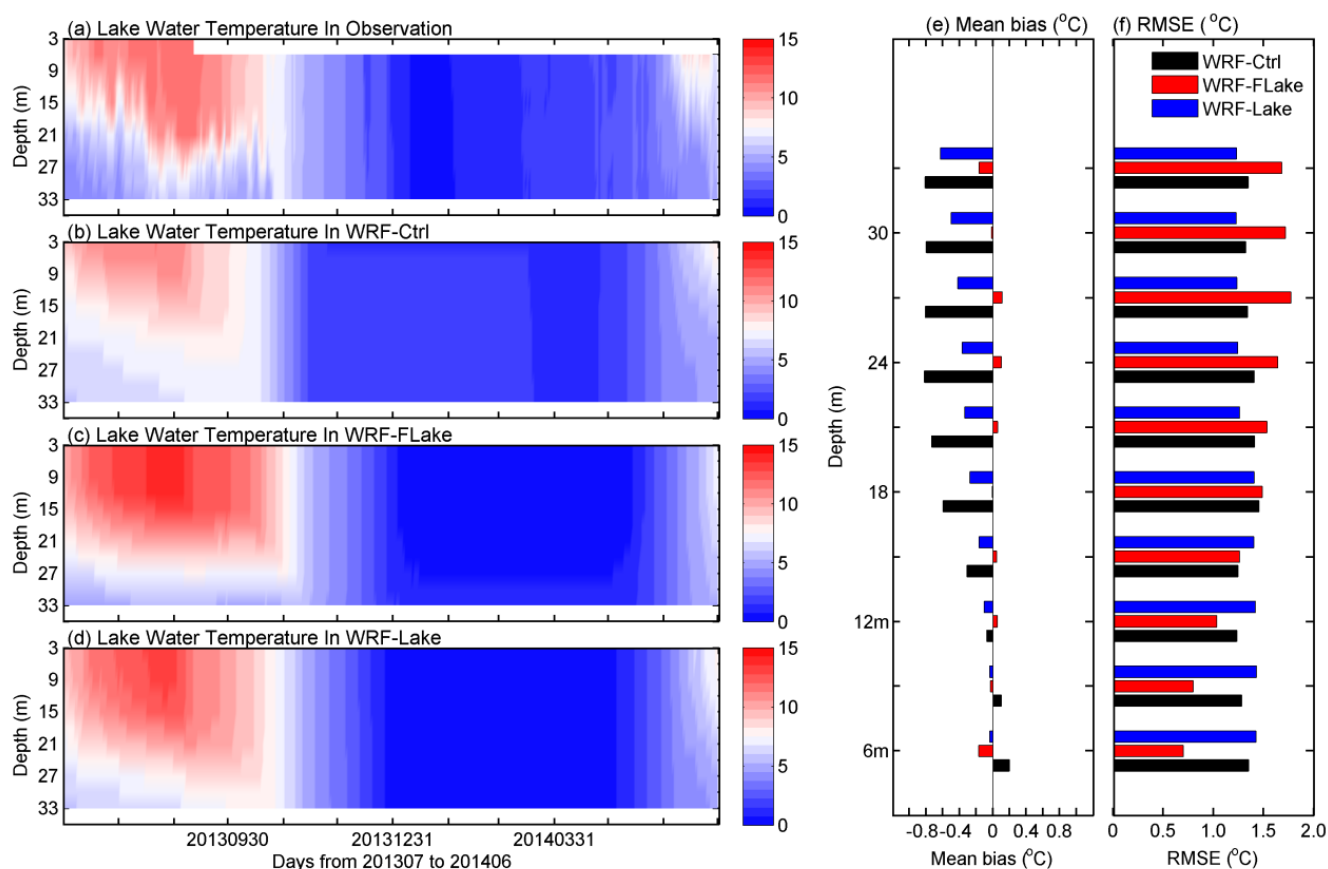when compared with the observations (Figure 4a).

265

Figure 4: Lake water temperature profiles in (a) station observations and each simulation (b: WRF-Ctrl, c: WRF-FLake and d: WRF-Lake) for the period of 1st July 2013 to 30nd June 2014, and (e-f) error metrics (mean bias and RMSE) at different depths.

270 **4.2 Lake ice phenology characteristics**

In this section, the simulated lake ice phenology is investigated, including the lake frozen fraction, ice thickness, freeze-up and break-up dates of the lake as a whole and for each lake grid, as well as the freeze-up duration. Freeze-up is defined as the

first day when lake ice occurs and ice-free days never occur in the following days (20 days for programming in this study) for each lake grid, while break-up is defined as the first day when ice-free occurs after reasonable number of ice-on days (20

275 days for programming in this study) for each lake grid. The lake frozen fraction is defined as the ratio of the number of ice-on grids to all grids. The lake freeze-up date is defined as the first day when the lake frozen fraction exceeds 90% and never falls below it within the next reasonable number of days (20 days for programming in this study), while the lake break-up date is defined as the first day of lake frozen fraction falls below 90% and never exists within the next reasonable number of days (20 days for programming in this study). For the calculation of freeze-up date and break-up date by MODIS, the

280 maximum LST in each grid is selected from the co-located 16 (4×4) MODIS pixels, which can preserve as much satellite information as we can to maintain maximally continuous time series within the grids. Even though, there are freeze-up date and break-up date in a considerable number of model grids that are still cannot be derived due to too much missing observations. The number of lake grids with missing values are even more when calculating the freeze-up durations by subtracting the break-up date and freeze-up date.

285 Following the method in *Zhou et al.* [2023], the ice phenology of lake Nam Co as a whole is investigated, including the frozen fraction, the mean ice thickness, and the penetrated shortwave radiation at the ice surface. Figure 5a shows the frozen fraction and mean ice thickness of Nam Co in each simulation. Based on MODIS, Nam Co generally freezes in January and breaks in late April (Figure 5a). For seasonality of lake ice phenology, both the WRF-FLake and the WRF-Lake runs generally show good agreement with MODIS, while WRF-Ctrl shows too-early freeze-up and break-up dates (Figure 5a).

290 For ice thickness, WRF-FLake simulates thicker ice than WRF-Lake, with maximum thicknesses of approximately 0.5 m and 0.4 m, respectively (Figure 5b). The reason could be attributed to more penetrating shortwave radiation at the ice surface (Figure 5c), and this part of the energy is more effective in contributing to ice melting in the model as interpreted by *Zhou et al.* [2023]. Compared with these two runs, WRF-Ctrl has much smaller ice thickness, which maintains a constant thickness during the main freeze-up period. This is because the thickness of the second layer was set to 4.0 m by default, which is too

295 deep and difficult to freeze. Additionally, the lake freeze-up and break-up dates, and freeze-up durations derived from each simulation are compared with those from MODIS, as shown in Table 1. Generally, WRF-Ctrl shows too-early freeze-up and break-up dates, while both revised models simulate the lake freeze-up and break-up dates with acceptable accuracy (errors within a few days), except for the break-up date in winter of 2014-2015 in WRF-Lake (Table 1). WRF-Ctrl shows too long freeze-up durations, which are effectively reduced in both WRF-FLake and WRF-Lake runs, though with too short freeze-up

300 durations in WRF-Lake (Table 1). This result indicates that, regarding lake freeze-up and break-up dates, the performances of the coupled model can be significantly improved by revising key parameters and improving key parameterizations in lake models.
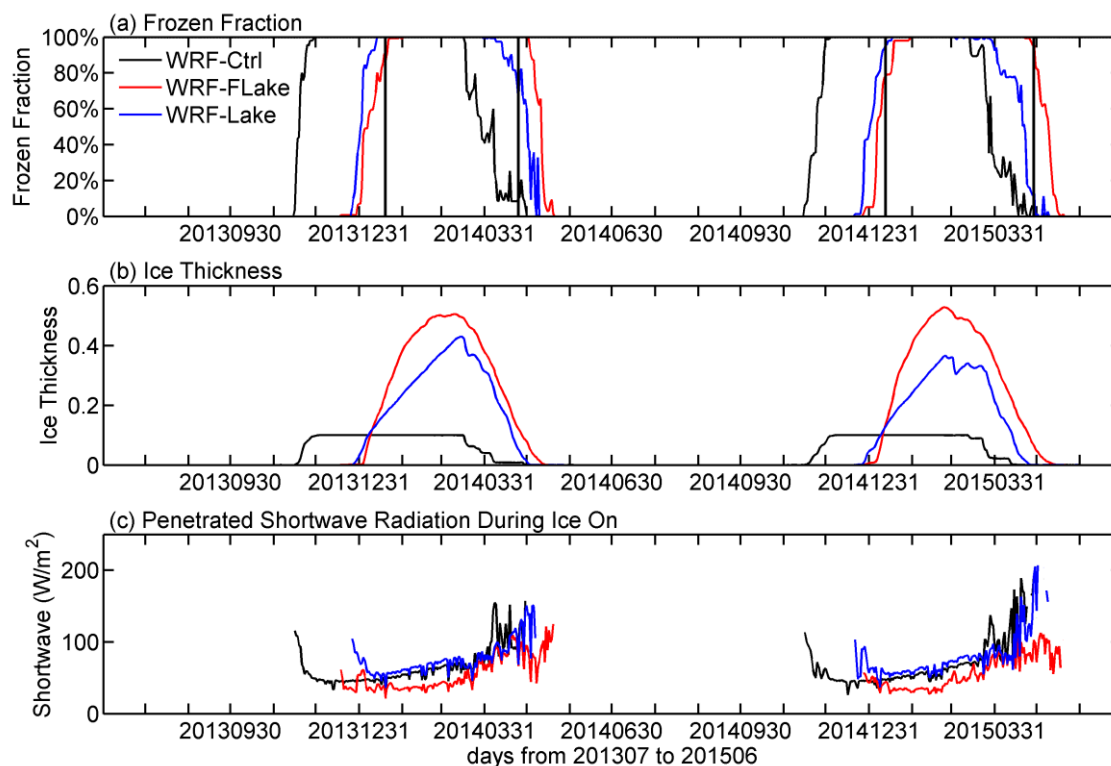
Figure 5: (a) Lake frozen fraction, (b) ice thickness, and (c) penetrated shortwave radiation (during the ice-on period) in each simulation.

Table 1: The comparisons of freeze-up dates, break-up dates and freeze-up durations (days) between each simulation and MODIS; the values indicate the number of days since 1st July of the corresponding year; the values in in parentheses indicate the errors of each simulation to MODIS; the Julian days of the freeze-up dates and break-up dates are provided for MODIS. Bold indicates a best performance.

	Freeze-up date 2013-204	Break-up date 2013-2014	Freeze-up duration (days) 2013-2014	Freeze-up date 2014-2015	Break-up date 2014-2015	Freeze-up duration (days) 2014-2015
WRF-Ctrl	146(-57)	261(-37)	115	152(-44)	267(-35)	115
WRF-FLake	**202(-1)**	307(+9)	105	202(+6)	**303(+1)**	**101**
WRF-	192(-11)	**294(-4)**	**102**	**194(-2)**	276(-26)	82

Lake						
MODIS	203(19th JAN)	298(24th APR)	95		196(12th JAN)	302(28th APR)	106

Figure 6 shows the spatial distribution of freeze-up date in each simulation. WRF-Ctrl show early freeze-up, while both revised models are consistent and show late freeze-up in eastern Nam Co, early freeze-up in the middle of the lake for winters of 2013-2014 and 2014-2015. Additionally, WRF-FLake shows slightly later freeze-up date than WRF-Lake. Figure 7 shows the spatial distribution of biases in freeze-up date in each simulation. Compared with MODIS, WRF-Ctrl shows systematically too early freeze-up date by more than 30 days, while the WRF-FLake and WRF-Lake runs show considerable smaller biases generally within ±20 days, with negative biases over the mid-western lake and positive biases over the eastern lake except for freeze-up date in 2014-2015 in the WRF-FLake.
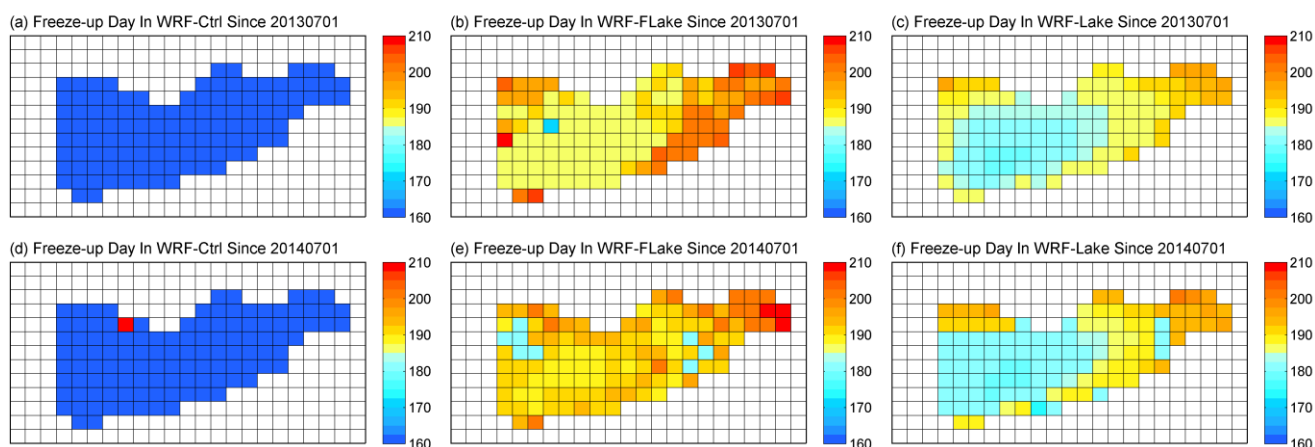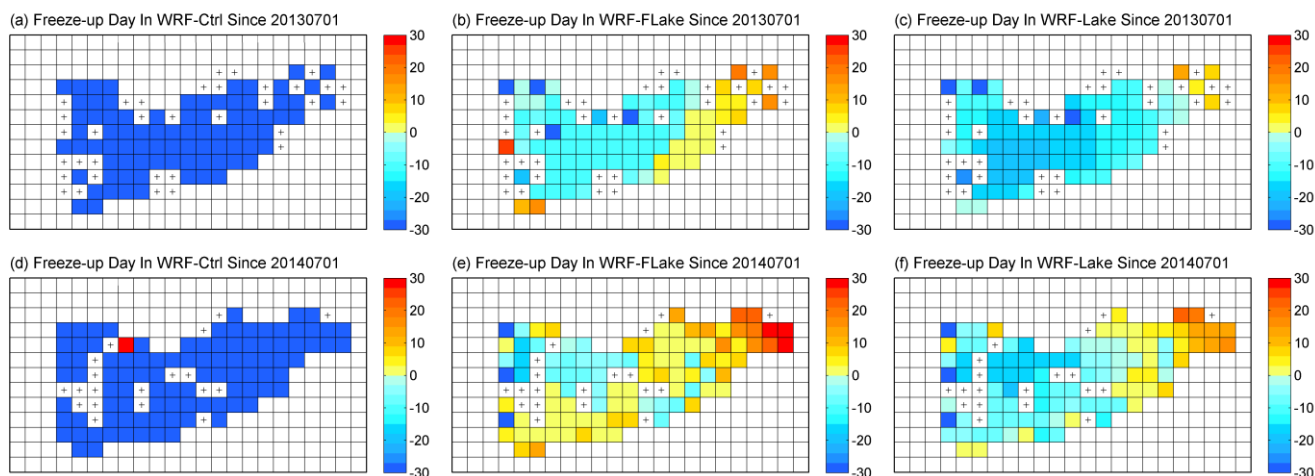

Figure 6: Spatial distribution of freeze-up date at Nam Co in each simulation in the winters of (a-c) 2013-2014 and (d-f) 2014-2015. The colour indicates the number of days since 1st July in the corresponding year.
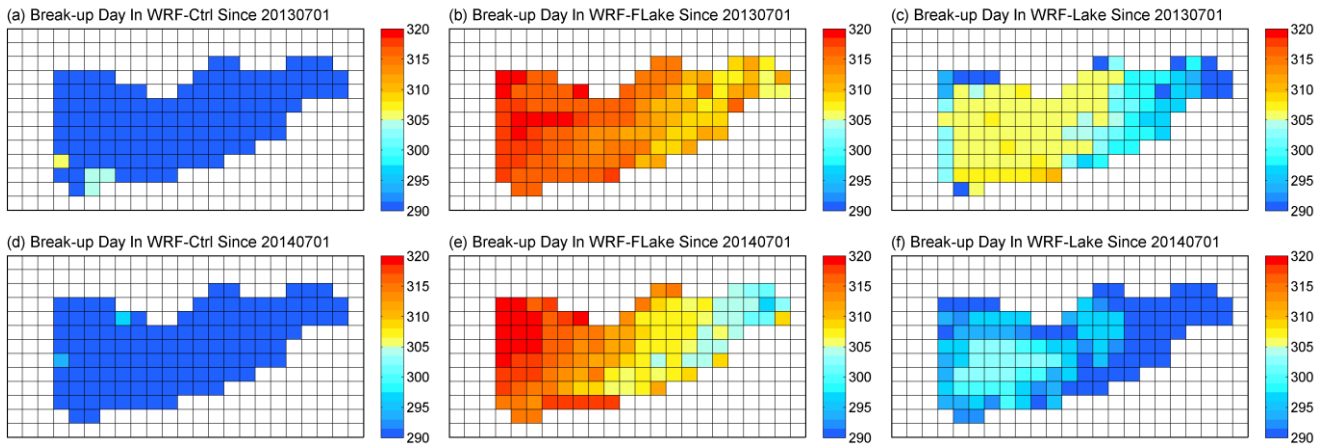
Figure 7: Spatial distribution of biases (days) in freeze-up date at Nam Co in each simulation in the winters of (a-c) 2013-2014 and (d-f) 2014-2015. The cross marks denote lake grids with missing observations in MODIS.
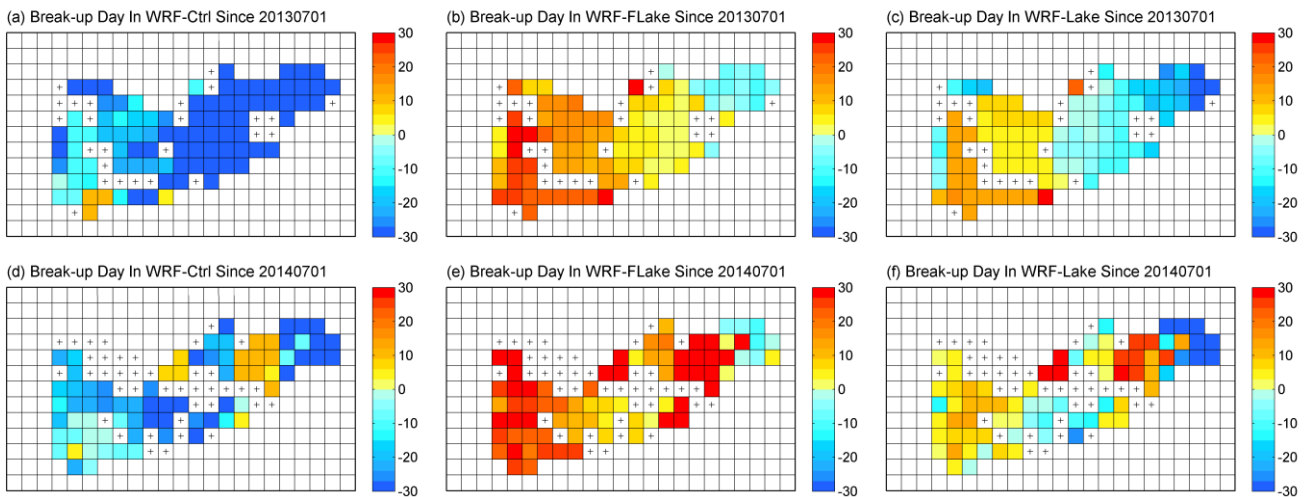
Figure 8 shows the spatial distribution of break-up date in each simulation. WRF-Ctrl shows early break-up, while both revised models show late break-up in western Nam Co, and early break-up in the middle for both springs of 2014 and 2015. The too-early break-up in WRF-Ctrl could be associated with the too-thin ice during freezing, and the ice-water phase change requires much less energy and thus a short time. Additionally, WRF-FLake shows a slightly later break-up date than WRF-Lake, which could be associated with the lake ice thickness in both runs. WRF-FLake has thicker ice during freezing and more energy is required for the ice-water phase change and thus it takes a longer time. Figure 9 shows the spatial distribution of biases in break-up date in each simulation. Compared with MODIS, WRF-Ctrl shows systematically too early break-up date by approximately 10-20 days, while the WRF-FLake and WRF-Lake runs show late break-up dates over the mid-western lake (more than 20 days and 0-10 days respectively) and early break-up dates over the eastern lake (-10-0 days and smaller than -20 days respectively).

15

Figure 8: Spatial distribution of break-up date at Nam Co in each simulation in the spring of (a-c) 2014 and (d-f) 2015, colour indicates the number of days since 1st July.

Figure 9: Spatial distribution of biases (days) in break-up date at Nam Co in each simulation in the spring of (a-c) 2014 and (d-f) 2015, colour indicates the number of days since 1st July. The cross marks denote lake grids with missing observations in MODIS.

Figure 10 shows the spatial distribution of freeze-up duration simulated by the two models. All models show the longest ice duration in the middle west of Nam Co, with WRF-Ctrl having the longest ice duration and WRF-FLake having a slightly longer freeze-up duration than that of WRF-Lake. The differences in the latter two runs could be associated with the differences in the parameterizations of shortwave processes when lake ice exists. Generally, the simulated ice duration is longer than 100 days and shorter than 140 days in both revised models. Figure 11 shows the spatial distribution of biases in

freeze-up duration in each simulation. Compared with MODIS, all the models show longer freeze-up durations over the mid-
355 western lake (approximately 10-20 days) and shorter freeze-up durations over the eastern corner of lake Nam Co
(approximately -20 --10 days). The too long freeze-up duration in WRF-Ctrl could be associated with the too early freeze-up
dates, while the too long freeze-up duration in WRF-FLake and WRF-Lake could be associated with the too late break-up
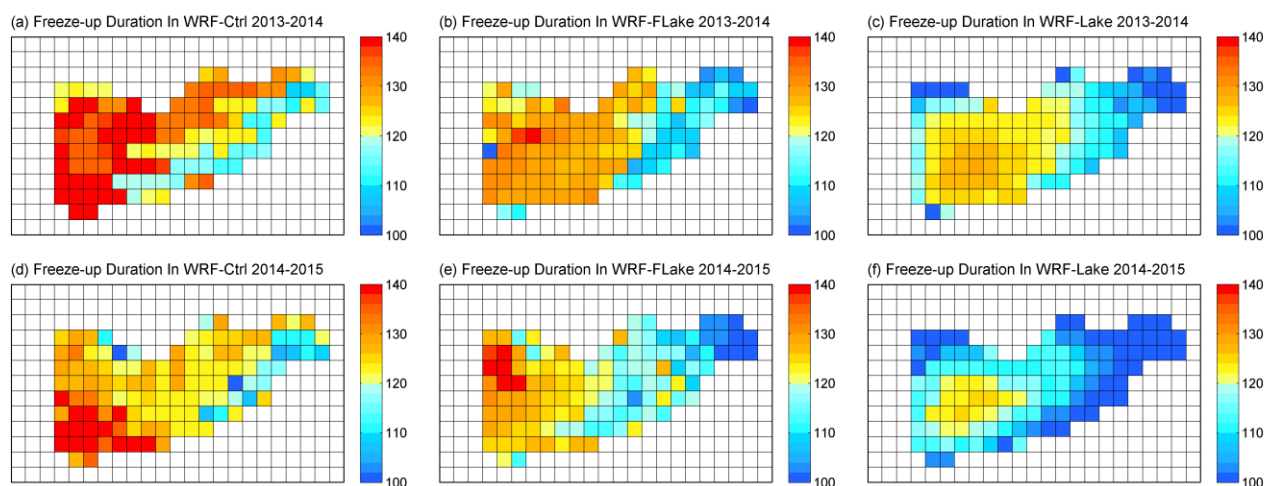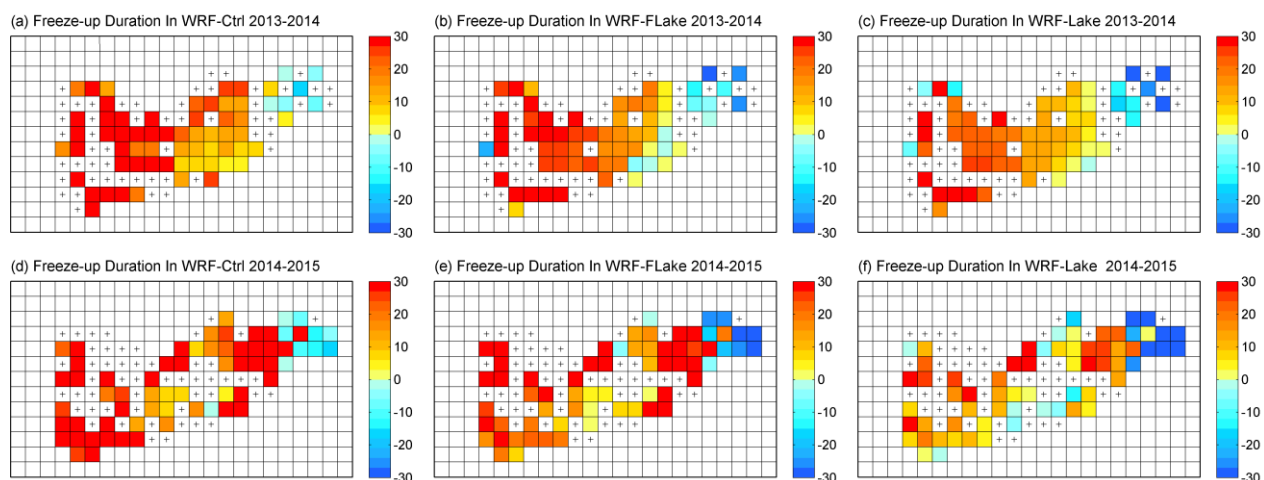dates.

360

Figure 10: Spatial distribution of freeze-up duration in each simulation in the periods of (a-c) 2013-2014 and (d-f) 2014-
2015, colour indicates the number of days during freeze-up.

365 **Figure 11:** Spatial distribution of biases (days) in freeze-up duration in each simulation in the periods of (a-c) 2013-2014
and (d-f) 2014-2015, colour indicates the number of days during freeze-up. The cross marks denote lake grids with missing
observations in MODIS.

17

Generally, the above evaluations demonstrate that with revisions of key parameters and improvements of key
370 parametrizations, associated with surface turbulent heat fluxes during ice-free period and associated with solar radiation
transfer during ice-on period, the updated model versions can significantly improve the simulation of ice phenology through
a better representation of lake energy processes. These improvements are observation and physics based, which is more
reasonable and more universal than using artificial scaling method as in Zhou et al. [2023]. For example, both WRF-FLake
and WRF-Lake models are improved by the same parameterization of water surface roughness length, demonstrating the
375 universality of this scheme as described in Eq.(4)-(5). Therefore, the current work provides a better model version for
weather and climate simulations over alpine lake regions. Nevertheless, there are still some limitations in describing model
physics, including both lake related and unrelated processes, which will be discussed in the next section.

5 Discussion

The above results and analysis showed that the two coupled atmosphere-lake models, WRF-FLake and WRF-Lake, with
380 proper revisions of key lake parameters and parameterizations can significantly improve the simulation of the lake ice
phenology characteristics. However, there might still be large uncertainties caused by the limitations of models' abilities in
depicting some physical processes, which will be discussed in this section.

In Section 4, some variables were evaluated, such as lake water temperature, lake freeze-up and break-up date, and freeze-up
durations. In this section, the spatial distributions of freeze-up date and break-up data derived from MODIS are presented for
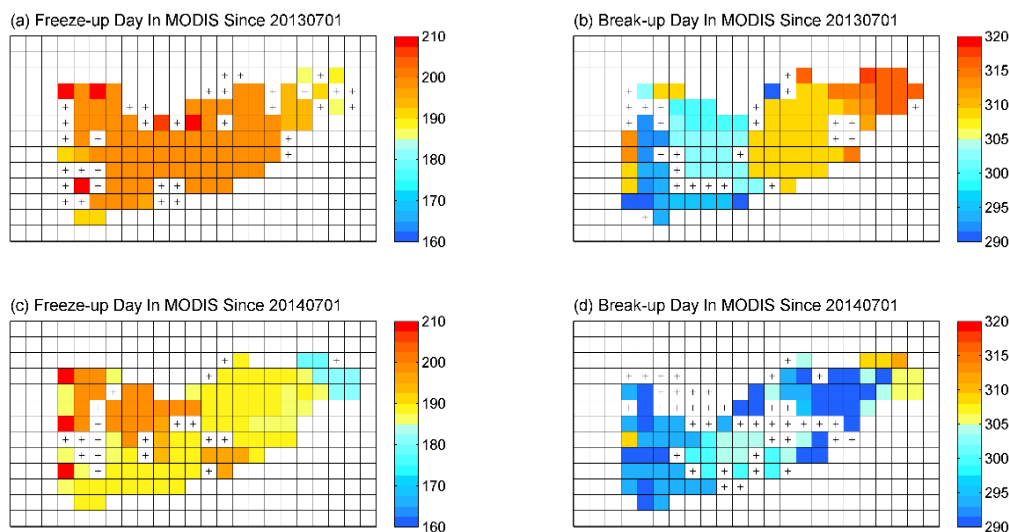385 a qualitative discussion in terms of west-east contrast.

Figure 12: Spatial distribution of freeze-up date (left) and break-up date (right) at Nam Co derived from MODIS in the period of (a-b) 2013-2014 and (c-d) 2014-2015. The cross marks denote lake grids with missing observations in MODIS.
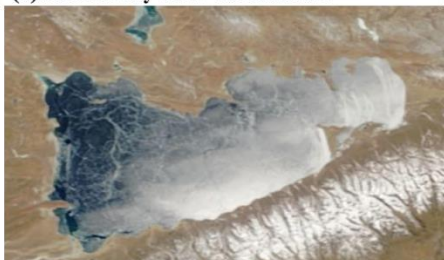
390

For freeze-up date, in both periods in 2013-2014 and 2014-2015, MODIS show early freeze-up in the east of Nam Co (Figure 12a, 12c), while models show early freeze-up in the middle-west (Figure 6). The identical lake depth for all grids can reflect the horizontal energy mixing associated with lake water circulation to a certain extent but may inevitably cause uncertainties in simulating the freeze-up date. Shallow water grids freeze-up earlier than deep water grids due to less water

395 and low heat capacity per unit area. Essentially, both lake models are one-dimensional models, and thus we speculate that the mismatch between the model and observation might also be associated with the lake water circulation that cannot be perfectly represented in the two lake models even with uniform depth. In cold seasons, the TP is dominated by prevailing westerlies. Before freeze-up, the wind blowing effect may lead to surface cooling water moving to the east and deep warm water moving to the west. A three-dimensional lake model is expected to solve this problem by depicting the horizontal lake

400 water circulation as demonstrated in *Wu et al.* [2021]. Nevertheless, a one-dimensional lake model is still commonly used in climate models when simulating atmosphere-lake processes, which highlights the importance of the current work.

For break-up date, in both periods in 2013-2014 and 2014-2015, MODIS show early break-up in the west (Figure 12b, 12d) while models show early break-up in eastern Nam Co (Figure 8). The freeze-up time in the models may play a role, because early freeze-up grids may accumulate thicker ice and vice versa for late freeze-up grids. Additionally, uncertainties

405 associated with snow cover at the lake ice surface play an important role through shortwave-albedo processes, as highlighted by *Li et al.* [2018] for offline models. In the simulations, there are nearly no snow cover (not shown). However, Figure 13a and 13b show that a considerable amount of snow covers the lake surface with inhomogeneous distribution from the west to the east of lake Nam Co, when looking at the images from the Earth Observing System Data and Information System (EOSDIS). Nearly no snow covers the west and a considerable amount of snow exists over the east. More snow can lead to a

410 high albedo and less shortwave absorption at the surface and thus have a cooling effect, which will delay ice melting. This contrast in snow cover between the model and observations is consistent and may partly explain the contrast in the spatial patterns of the lake break-up date over Nam Co. Obviously, both coupled models have the disadvantage of simulating the snow cover over lake ice. In the simulations, nearly no precipitation was simulated at lake grids during freeze-up (not shown). Frozen and smooth surfaces are not favourable for triggering atmospheric convection and snowfall. Therefore, we

415 speculate that the snow covers at lake ice surface, as shown in the sky view images, might be associated with grid-scale snow dynamic processes like blowing snow during snowfall (during snowflake descent) and after snowfall (at land/lake surface). With rough surfaces such as bare ground or vegetated land, the scale of blowing snow might be limited to a small scale and can be parameterized by a scheme such as the one introduced by *Xie et al.* [2019]. However, for a smooth surface, such as the ice surface in the current work, the scale of blowing snow can be much larger and the applicability of such a

420 scheme needs to be investigated. Furthermore, lakes generally have lower elevations than the surrounding land and are beneficial for snow accumulation, especially during snowfall.

Figure 13: Satellite sky view images from EOSDIS Worldview on typical lake ice-on days in (a) 20140315 and (b)
425   20150226 (right).

Additionally, other lake processes can also bring uncertainties in simulating the lake ice phenology. For example, during ice-
covered period, the shortwave radiation absorbed by lake water under ice can increase the water temperature to more than
the freezing point [*Kirillin et al.*, 2021; *La et al.*, 2021; *Wang et al.*, 2022] and delay ice melting by temporally storing the
430   energy in water instead of being used immediately for ice melting. These uncertainties in describing lake-related processes
bring considerable inconsistencies between models and observations associated with ice phenology. Simultaneously, they
also bring great challenges in model applications and developments, especially for deep alpine lake regions.

6 Summary and remarks

In this study, the WRF model coupled with two lake models, the FLake model and the default simplified CLM lake model
435   (namely WRF-FLake and WRF-Lake, respectively), have been applied to simulate lake ice phenology in a typical alpine
lake located in the central TP.
With improvements of momentum, hydraulic and thermal roughness length parameterizations, both the WRF-FLake and the
WRF-Lake models reasonably simulated the lake water temperature compared with MODIS and station observations. Water
temperature represents the lake energy storage, and therefore, the lake freeze-up date in both models was reasonably
440   simulated compared with MODIS. With revisions of key parameters and improvements of key parameterizations associated
with the shortwave radiation transfer both the WRF-FLake and the WRF-Lake models generally simulated the lake break-up

date well. These improvements are observation and physics based, which are more reasonable and more universal than using artificial scaling method as in *Zhou et al.* [2023]. Compared with WRF coupled with the unrevised default lake model, the simulation of lake ice phenology was significantly improved by WRF coupled with both the improved lake models.

445 Therefore, the main results and findings of this work can provide a good reference for climate model applications and the improved model also has practical application prospects over the alpine lake covered regions.

However, considerable errors still exist in simulating the spatial patterns of freeze-up and break-up dates. These errors could come from the disadvantages of the model in representing some key lake physics such as nonuniform lake depth, lake water circulation, shortwave heating effect on water underneath lake ice, and atmospheric processes such as grid-scale blowing

450 snow, indicating that more substantial work is required to improve the lake physical processes in climate models. Nevertheless, our work can provide a better model version compared with the default WRF model and the discussions are expected to provide new implications for advancing lake ice associated processes in coupled atmosphere-lake models in the future.

Code and data availability

455 The model code and simulation data is available online at https://doi.org/10.17632/bpjcbdkj4c.1.

Author contributions

Author contributions: Conceptualization: Xu Zhou and Binbin Wang; Data curation: Xu Zhou and Lazhu; Formal analysis, Validation and Visualization: Xu Zhou; Funding acquisition: Xu Zhou, Binbin Wang, Lazhu and Kun Yang; Supervision: Kun Yang; Roles/Writing - original draft: Xu Zhou and Binbin Wang; and Writing - review & editing: All authors.

460 **Competing interests**

The authors declare that there are no conflicts of interest.

Acknowledgments

References

Dai, Y., Wei, N., Huang, A., Zhu, S., Shangguan, W., Yuan, H., Zhang, S., and Liu, S.: The lake scheme of the Common Land Model and
470 its performance evaluation, Chinese Science Bulletin, *63*(28-29), 3002-3021, doi:10.1360/N972018-00609, 2018.

Dai, Y. F., Wang, L., Yao, T. D., Li, X. Y., Zhu, L. J., and Zhang, X. W.: Observed and Simulated Lake Effect Precipitation Over the Tibetan Plateau: An Initial Study at Nam Co Lake, J Geophys Res-Atmos, *123*(13), 6746-6759, doi:10.1029/2018jd028330, 2018.

Dee, D. P., et al.: The ERA-Interim reanalysis: configuration and performance of the data assimilation system, Quarterly Journal of the Royal Meteorological Society, *137*(656), 553-597, doi:10.1002/qj.828, 2011.

475   Dudhia, J.: Numerical Study of Convection Observed during the Winter Monsoon Experiment Using a Mesoscale Two-Dimensional Model, *J Atmos Sci*, *46*(20), 3077-3107, doi:10.1175/1520-0469(1989)046<3077:Nsocod>2.0.Co;2, 1989.

Efremova, T. V., and Pal'shin, N. I.: Ice Phenomena Terms on the Water Bodies of Northwestern Russia, *Russ Meteorol Hydro+*, *36*(8), 559-565, doi:10.3103/S1068373911080085, 2011.

Gu, H. P., Jin, J. M., Wu, Y. H., Ek, M. B., and Subin, Z. M.: Calibration and validation of lake surface temperature simulations with the
480   coupled WRF-lake model, *Climatic Change*, *129*(3-4), 471-483, doi:10.1007/s10584-013-0978-y, 2015.

Guo, Y. H., Zhang, Y. S., Ma, N., Song, H. T., and Gao H. F.: Quantifying Surface Energy Fluxes and Evaporation over a Significant Expanding Endorheic Lake in the Central Tibetan Plateau, *J Meteorol Soc Jpn*, *94*(5), 453-465, doi:10.2151/jmsj.2016-023, 2016.

Huang, A. N., et al.: Evaluating and Improving the Performance of Three 1-D Lake Models in a Large Deep Lake of the Central Tibetan Plateau, *J Geophys Res-Atmos*, *124*(6), 3143-3167, doi:10.1029/2018jd029610, 2019.

485   Huang, W. F., Cheng, B., Zhang, J. R., Zhang, Z., Vihma, T., Li, Z. J., and Niu, F. J.: Modeling experiments on seasonal lake ice mass and energy balance in the Qinghai-Tibet Plateau: a case study, *Hydrol Earth Syst Sc*, *23*(4), 2173-2186, doi:10.5194/hess-23-2173-2019, 2019.

Huang, W. F., Zhao, W., Zhang, C., Lepparanta, M., Li, Z. J., Li, R., and Lin, Z. J.: Sunlight penetration dominates the thermal regime and energetics of a shallow ice-covered lake in arid climate, *Cryosphere*, *16*(5), 1793-1806, doi:10.5194/tc-16-1793-2022, 2022.

Janjic, Z.: Nonsingular implementation of the Mellor- Yamada level 2.5 scheme in the NCEP mesoscale model. National Centers for
490   Environmental Prediction Office, *Tech. Rep.*, *437*, 2001.

Kirillin, G., et al.: Physics of seasonally ice-covered lakes: a review, *Aquat Sci*, *74*(4), 659-682, doi:10.1007/s00027-012-0279-y, 2012.

Kirillin, G. B., Shatwell, T., and Wen, L. J.: Ice-Covered Lakes of Tibetan Plateau as Solar Heat Collectors, *Geophys Res Lett*, *48*(14), doi:10.1029/2021GL093429, 2021.

La, Z., Yang, K., Qin, J., Hou, J. Z., Lei, Y. N., Wang, J. B., Huang, A. N., Chen, Y. Y., Ding, B. H., and Li, X.: A Strict Validation of
495   MODIS Lake Surface Water Temperature on the Tibetan Plateau, *Remote Sens-Basel*, *14*(21), doi:ARTN 545410.3390/rs14215454, 2022.

La, Z., Yang, K., Wang, J. B., Lei, Y. B., Chen, Y. Y., Zhu, L. P., Ding, B. H., and Qin, J.: Quantifying evaporation and its decadal change for Lake Nam Co, central Tibetan Plateau, *J Geophys Res-Atmos*, *121*(13), 7578-7591, doi:10.1002/2015jd024523, 2016.

Lazhu, Yang, K., Hou, J. Z., Wang, J. B., Lei, Y. B., Zhu, L. P., Chen, Y. Y., Wang, M. D., and He, X. G.: A new finding on the
500   prevalence of rapid water warming during lake ice melting on the Tibetan Plateau, *Sci Bull*, *66*(23), 2358-2361, doi:10.1016/j.scib.2021.07.022, 2021.

Lei, Y. B., Yang, K., Wang, B., Sheng, Y. W., Bird, B. W., Zhang, G. Q., and Tian, L. D.: Response of inland lake dynamics over the Tibetan Plateau to climate change, *Climatic Change*, *125*(2), 281-290, doi:10.1007/s10584-014-1175-3, 2014.

505 Lei, Y. B., Yao, T. D., Bird, B. W., Yang, K., Zhai, J. Q., and Sheng, Y. W.: Coherent lake growth on the central Tibetan Plateau since the 1970s: Characterization and attribution, *J Hydrol*, *483*, 61-67, doi:10.1016/j.jhydrol.2013.01.003, 2013.

Lei, Y. B., et al.: An integrated investigation of lake storage and water level changes in the Paiku Co basin, central Himalayas, *J Hydrol*, *562*, 599-608, doi:10.1016/j.jhydrol.2018.05.040, 2018.

Li, X. Y., et al.: Evaporation and surface energy budget over the largest high-altitude saline lake on the Qinghai-Tibet Plateau, *J Geophys Res-Atmos*, *121*(18), 10470-10485, doi:10.1002/2016jd025027, 2016.

510 Li, Z. G., Ao, Y. H., Lyu, S., Lang, J. H., Wen, L. J., Stepanenko, V., Meng, X. H., and Zhao, L.: Investigation of the ice surface albedo in the Tibetan Plateau lakes based on the field observation and MODIS products, *J Glaciol*, *64*(245), 506-516, doi:10.1017/jog.2018.35, 2018).

Li, Z. G., Lyu, S. H., Wen, L. J., Zhao, L., Ao, Y. H., and Meng X. H.: Study of freeze-thaw cycle and key radiation transfer parameters in a Tibetan Plateau lake using LAKE2.0 model and field observations, *J Glaciol*, *67*(261), 91-106, doi:10.1017/jog.2020.87, 2021.

515 Ma, X. G., Yang, K., La, Z., Lu, H., Jiang, Y. Z., Zhou, X., Yao, X. N., and Li, X.: Importance of Parameterizing Lake Surface and Internal Thermal Processes in WRF for Simulating Freeze Onset of an Alpine Deep Lake, *J Geophys Res-Atmos*, *127*(18), doi:10.1029/2022JD036759, 2022.

Mellor, G. L., and Yamada, T.: Hierarchy of Turbulence Closure Models for Planetary Boundary-Layers, *J Atmos Sci*, *31*(7), 1791-1806, doi:10.1175/1520-0469(1974)031<1791:Ahotcm>2.0.Co;2, 1974.

520 Mironov, D.: Parameterization of Lakes in Numerical Weather Prediction. Description of a Lake Model.*Rep,* 2008.

Mlawer, E. J., Taubman, S. J., Brown, P. D., Iacono, M. J., and Clough, S. A.: Radiative transfer for inhomogeneous atmospheres: RRTM, a validated correlated-k model for the longwave, *J Geophys Res-Atmos*, *102*(D14), 16663-16682, doi:10.1029/97jd00237, 1997.

Niu, G. Y., et al.: The community Noah land surface model with multiparameterization options (Noah-MP): 1. Model description and evaluation with local-scale measurements, *J Geophys Res-Atmos*, *116*, doi:10.1029/2010jd015139, 2011.

525 Skamarock, W. C., Klemp, J. B., Gill, D. O., Barker, D. M., Duda, M. G., Huang, X., Wang, W., and Powers, J. G.: A description of the advanced research WRF model version 3*Rep.*, National Center for Atmospheric Research, National Center for Atmospheric Research: Boulder, CO, USA, 145, 2008.

Su, D. S., Wen, L. J., Gao, X. Q., Lepparanta, M., Song, X. Y., Shi, Q. Q., and Kirillin, G.: Effects of the Largest Lake of the Tibetan Plateau on the Regional Climate, *J Geophys Res-Atmos*, *125*(22), doi:10.1029/2020JD033396, 2020.

530 Thompson, G., Field, P. R., Rasmussen, R. M., and Hall, W. D.: Explicit Forecasts of Winter Precipitation Using an Improved Bulk Microphysics Scheme. Part II: Implementation of a New Snow Parameterization, *Mon Weather Rev*, *136*(12), 5095-5115, doi:10.1175/2008mwr2387.1, 2008.

Wan, Z., Hook, S., and Hulley, G.: MYD11C3 MODIS/Aqua Land Surface Temperature/Emissivity Monthly L3 Global 0.05Deg CMG V006 [Dataset], edited, doi:10.5067/MODIS/MYD11C3.006, 2015.

535 Wang, B. B., Ma, Y. M., Wang, Y., Su, Z. B., and Ma, W.: Significant differences exist in lake-atmosphere interactions and the evaporation rates of high-elevation small and large lakes, *J Hydrol*, *573*, 220-234, doi:10.1016/j.jhydrol.2019.03.066, 2019.

Wang, J. B.: Water temperature observation data at Nam Co Lake in Tibet (2011-2014), edited by National Tibetan Plateau Data Center, National Tibetan Plateau Data Center, doi:10.11888/Hydro.tpdc.270332, 2020.

Wang, J. B., Huang, L., Ju, J. T., Daut, G., Wang, Y., Ma, Q. F., Zhu, L. P., Haberzettl, T., Baade, J., andMausbacher, R.: Spatial and 540 temporal variations in water temperature in a high-altitude deep dimictic mountain lake (Nam Co), central Tibetan Plateau, *J Great Lakes Res*, *45*(2), 212-223, doi:10.1016/j.jglr.2018.12.005, 2019.

Wang, J. B., Zhu, L. P., Daut, G., Ju, J. T., Lin, X., Wang, Y., and Zhen X. L.:, Investigation of bathymetry and water quality of Lake Nam Co, the largest lake on the central Tibetan Plateau, China, *Limnology*, *10*(2), 149-158, doi:10.1007/s10201-009-0266-8, 2009.

Wang, M. X., Wen, L. J., Li, Z. G., Lepparanta, M., Stepanenko, V., Zhao, Y. X., Niu, R. J., Yang, Y. Y., and Kirillin, G.: Mechanisms 545 and effects of under-ice warming water in Ngoring Lake of Qinghai-Tibet Plateau, *Cryosphere*, *16*(9), 3635-3648, doi:10.5194/tc-16-3635-2022, 2022.

Wen, L. J., Lyu, S. H., Kirillin, G., Li, Z. G., and Zhao L: Air-lake boundary layer and performance of a simple lake parameterization scheme over the Tibetan highlands, *Tellus A*, *68*, doi:10.3402/tellusa.v68.31091, 2016).

Wu, Y., Huang, A. N., Lu, Y. Y., Lazhu, Yang, X. Y., Qiu, B., Zhang, Z. Q., and Zhang, X. D.: Numerical Study of the Thermal 550 Structure and Circulation in a Large anal Deep Dimictic Lake Over Tibetan Plateau, *J Geophys Res-Oceans*, *126*(10), doi:10.1029/2021JC017517, 2021.

Wu, Y., et al.: Numerical study on the climatic effect of the lake clusters over Tibetan Plateau in summer, *Clim Dynam*, *53*(9-10), 5215-5236, doi:10.1007/s00382-019-04856-4, 2019.

Xie, Z., Hu, Z., Ma, Y., Sun, G., Gu, L., Liu, S., Wang, Y., Zheng, H., and Ma, W.: Modeling Blowing Snow Over the Tibetan Plateau 555 With the Community Land Model: Method and Preliminary Evaluation, *Journal of Geophysical Research: Atmospheres*, *124*(16), 9332-9355, doi:10.1029/2019JD030684, 2019.

Xu, X. D., Lu, C. G., Shi, X. H., and Gao, S. T.: World water tower: An atmospheric perspective, *Geophys Res Lett*, *35*(20), doi:10.1029/2008gl035867, 2008.

Yang, X. Y., Wen, J., Huang, A. N., Lu, Y. Q., Meng, X. H., Zhao, Y., Wang, Y. R., and Meng, L. X.: Short-Term Climatic Effect of 560 Gyaring and Ngoring Lakes in the Yellow River Source Area, China, *Front Earth Sc-Switz*, *9*, doi:10.3389/feart.2021.770757, 2022.

Yang, Z. L.: The community Noah land surface model with multiparameterization options (Noah-MP): 2. Evaluation over global river basins, *J Geophys Res-Atmos*, *116*, doi:10.1029/2010jd015140, 2011.

Yao, X. N., Yang, K., Letu, H., Zhou, X, Wang, Y., Ma, X., Lu, H. and La, Z.: Observation and Process Understanding of Typical Cloud Holes Above Lakes Over the Tibetan Plateau, *Journal of Geophysical Research: Atmospheres*, *128*(13), e2023JD038617, 565 doi:10.1029/2023JD038617, 2023.

Yao, X. N., Yang, K., Zhou, X., Wang, Y., Lazhu, Chen, Y. Y., and Lu, H: Surface friction contrast between water body and land enhances precipitation downwind of a large lake in Tibet, *Clim Dynam*, *56*(7-8), 2113-2126, doi:10.1007/s00382-020-05575-x, 2021.

Zhang, G. Q., Luo, W., Chen, W. F., and Zheng, G. X.: A robust but variable lake expansion on the Tibetan Plateau, *Sci Bull*, *64*(18), 1306-1309, doi:10.1016/j.scib.2019.07.018, 2019.

570   Zhang, G. Q., Yao, T. D., Xie, H. J., Qin, J., Ye, Q. H., Dai, Y. F., and Guo, R. F.: Estimating surface temperature changes of lakes in the Tibetan Plateau using MODIS LST data, *J Geophys Res-Atmos*, *119*(14), 8552-8567, doi:10.1002/2014jd021615, 2014.

Zhang, G. Q., et al.: Response of Tibetan Plateau lakes to climate change: Trends, patterns, and mechanisms, *Earth-Sci Rev*, *208*, doi:10.1016/j.earscirev.2020.103269, 2020.

Zhao, Z. Z., Huang, A. N., Ma, W. Q., Wu, Y., Wen, L. J., Lazhu, and Gu, C. L.: Effects of Lake Nam Co and Surrounding Terrain on
575   Extreme Precipitation Over Nam Co Basin, Tibetan Plateau: A Case Study, *J Geophys Res-Atmos*, *127*(10), doi:10.1029/2021JD036190, 2022.

Zhou, X., Beljaars, A., Wang, Y., Huang, B., Lin, C., Chen, Y., and Wu, H.: Evaluation of WRF Simulations With Different Selections of Subgrid Orographic Drag Over the Tibetan Plateau, *J Geophys Res-Atmos*, *122*(18), 9759-9772, doi:10.1002/2017jd027212, 2017.

Zhou, X., Lazhu, Yao, X., and Wang, B.: Understanding two key processes associated with alpine lake ice phenology using a coupled
580   atmosphere-lake model, *Journal of Hydrology: Regional Studies*, *46*, 101334, doi:10.1016/j.ejrh.2023.101334, 2023.

Zhou, X., Yang, K., Ouyang, L., Wang, Y., Jiang, Y. Z., Li, X., Chen, D. L., and Prein, A.: Added value of kilometer-scale modeling over the third pole region: a CORDEX-CPTP pilot study, *Clim Dynam*, *57*(7-8), 1673-1687, doi:10.1007/s00382-021-05653-8, 2021.

25